The crystal chemistry of doyleite, $Al(OH)_3$

G. R. Clark

University of Auckland, Department of Chemistry, Private Bag, 92019 Auckland, New Zealand

K. A. Rodgers*

University of Auckland, Department of Geology, Private Bag, 92019 Auckland, New Zealand

and G. S. Henderson

University of Toronto, Department of Geology, 22 Russell Street, Toronto, Ontario M5S 3B1, Canada

Received April 7, 1997; accepted August 13, 1997

Abstract. The structure of doyleite, a rare polymorph of $Al(OH)_3$, has been determined by a three-dimensional single-crystal diffraction study as triclinic, space group $P\bar{1}$, $a = 4.9997(8)$ Å, $b = 5.1681(6)$ Å, $c = 4.9832(6)$ Å, $\alpha = 97.444(10)°$, $\beta = 118.688(12)°$, $\gamma = 104.661(12)°$, $V = 104.39(3)$ Å^3, $Z = 2$. Doyleite has a similar bilayer structure to the other modifications of $Al(OH)_3$, comprising double layers of *hcp* O atoms with Al atoms occupying two-thirds of the octahedral interstices but is distinct from the other forms in its lateral displacement of adjacent layers and in aspects of the hydrogen bonding pattern. A good correspondence exists between the calculated structure and AFM images of doyleite's (010) surface. The OH-stretching Raman spectrum shows a single broad band centred near 3345 cm^{-1} with a weaker shoulder at 3615 cm^{-1} in some spectra. Intra-layer interactions between hydroxyl groups appear to involve limited, if any, bonding between a hydrogen and the next-nearest-neighbour oxygen and show no Raman scattering, in contrast to other $Al(OH)_3$ polymorphs. The ~100 cm^{-1} width of doyleite's OH-stretching band is taken as describing the time-averaged hydrogen bond-strength distribution throughout the crystal, with a continuous range of bond strengths consequential upon interchanging positional disorder of the hydrogen atoms and their varying involvement in interplane hydrogen bonds.

Introduction

Doyleite is a triclinic polymorph of $Al(OH)_3$. It was first described by Chao, Baker, Sabina and Roberts (1985) from albitite veins in a nepheline syenite occurring at Mont St. Hilaire, Quebec. These authors determined, from zonal precession photographs, its structural distinction from the other $Al(OH)_3$ minerals, gibbsite, bayerite and nordstrandite, and they deduced that the stacking of the layers was the *-ABAB-* of bayerite, rather than the *-ABBAABBA-* of gibbsite, with a concomitant lateral displacement of successive layers. Chao et al. stated, without providing structural data, that doyleite differed from other $Al(OH)_3$ polymorphs in having only one crystallographically independent $Al(OH)_6$ octahedron. In the other polymorphs, two distinct octahedra are present. The authors argued that a consequence of this difference could be seen in the infrared absorption spectra where that of doyleite is characterised by a simplicity that contrasts with the numerous well-defined bands present in the spectra of gibbsite and nordstrandite. The Raman spectra of the different polymorphs show similar contrasts (Rodgers, 1992) such that the doyleite structure is readily identified in the presence of the other polymorphs.

Nonetheless, doubts have been expressed as to the validity of doyleite as a true modification of $Al(OH)_3$ (Wefers and Misra, 1987). In order to verify the legitimacy of doyleite as a mineral species and to ascertain its precise structural distinction from the other natural $Al(OH)_3$ polymorphs, a full three-dimensional single crystal diffraction study of doyleite has been undertaken and the deduced structure compared with results of Atomic Force Microscopy (Enzel and Henderson, 1996) and Laser Raman Spectroscopy (Rodgers, 1992).

X-ray study

The Royal Ontario Museum generously loaned a small portion of the type specimen of doyleite, M41025, from which one small wedge-shaped plate of suitable size and quality was extracted. This crystal diffracted very strongly and the entire reciprocal lattice was recorded to $\theta = 35°$, with 92% of all reflections exceeding the observed criterion of $F_o > 4\sigma(F_o)$. Data were collected on an Enraf-Nonius CAD-4 diffractometer using graphite-monochromated MoK_α radiation. Unit cell dimensions were determined from the goniometer setting angles of 25 reflections in the

* Correspondence author (e-mail: ka.rodgers@auckland.ac.nz)

theta range 7.4°−18.3°. An empirical absorption correction was applied from psi-scan data (North, Phillips and Mathews, 1968) as well as Lorentz and polarisation corrections.

The Al and O positions were solved from the Patterson map using SHELXS-86 (Sheldrick, 1986). After initial refinement, a difference electron density map phased by the Al and O atoms was computed in an attempt to locate the three hydrogen atoms which are expected to lie either in or perpendicular to the plane of the oxygen atoms. The most obvious feature of the map was three large peaks situated approximately perpendicular to the plane of the oxygens, and from the distances, clearly involved in hydrogen bonds to oxygen atoms in adjacent layers. However, if these indicate hydrogen positions, their disposition is in fundamental conflict with the crystallographic symmetry. This is because the hydrogen atoms projecting down from one layer of oxygens bump into the hydrogens projecting up from the layer below. Only half of these hydrogen positions can be filled at any one time, and the observed electron density difference map is a time-averaged image of local symmetries for the total spread of mosaic blocks throughout the whole crystal. The overall effect is that of positional disorder of these hydrogen atoms in their hydrogen bonds: i.e. half of the time O−H . . . O and half of the time O . . . H−O. The arrangement of the inter-layer hydrogen bonds are shown schematically in Fig. 1.

This effect is reminiscent of the split deuterium positions in the neutron diffraction study of the heavy ice structure (Peterson and Levy, 1957) where, on average, the hydrogen atom is attached to each of the two oxygen atoms half of the time. In the case of doyleite, the hydrogen atoms between the layers are related through crystallographic centres of symmetry to an equivalent peak in a neighbouring asymmetric unit. Because of the location of the centres of symmetry, the specific relationships are:

O(1)−H(1) . . . O(2′)	O(1) . . . H(2)−O(2′)
O(2)−H(2) . . . O(1′)	O(2) . . . H(2)−O(1′)
O(3)−H(3) . . . O(3′)	O(3) . . . H(3)−O(3′)

It is concluded therefore, that for one half of the time one of the hydrogen atoms on each oxygen atom is involved in an inter-layer hydrogen bond.

The second feature of the difference electron density map is three less intense and quite diffuse peaks situated approximately within the oxygen plane. They are disposed towards the centre of the triangle of three oxygen atoms and indicate the most probable locations of the remaining three half-hydrogen atoms. We infer from the diffuse nature of this set of electron densities that these intra-layer hydrogen atoms are not involved in significant hydrogen bonds and that their exact position in any individual mosaic block is dependent upon the local placement of the hydrogens on the other two oxygens. Thus, on average, the hydrogen on each oxygen can be either participating in an inter-layer hydrogen bond or else occupying a position approximately within the oxygen layer.

In order to model this arrangement, two sets of half-hydrogen atoms have been included for each oxygen. Hydrogens "A" are those involved in the inter-layer hydrogen bonds. Their positions are uniquely determined and they were assigned 0.5 occupancy with an isotropic temperature factor of 0.02. Hydrogens "B" are those situated within the layers. Their positions were arbitrarily selected on the basis of the best peak position coupled with a sensible O−H distance and they were assigned an occupancy of 0.5 with a higher isotropic temperature factor of 0.05 to more closely relate to the lower electron density in the map. Refinement of the Al and O atoms with anisotropic

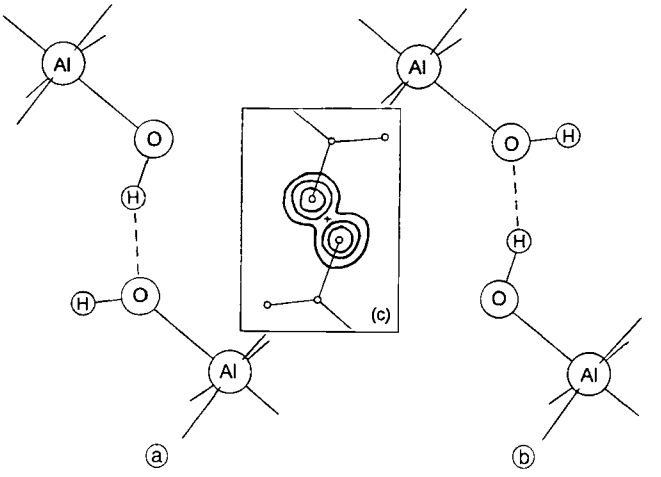

Fig. 1. Schematic representation of inter-layer hydrogen bonding in doyleite as interpreted from the difference electron density map (**c**). The crystallographic centre of symmetry is depicted as +. Diagrams (**a**) and (**b**) represent local arrangements involving one of the pairs of oxygen atoms. Similar local arrangements apply to other pairs of oxygen atoms involved in inter-layer hydrogen bonding.

Table 1. Experimental conditions for the structure determination of doyleite, $Al(OH)_3$.

Empirical formula	H_3AlO_3
Colour, habit and size	colourless platelets, 0.29 × 0.20 × 0.06 mm
Formula weight	78.00
Crystal system, space group; Z	triclinic, $P\bar{1}$; 2
Unit cell dimensions	$a = 4.9997(8)$ Å, $b = 5.1681(6)$ Å, $c = 4.9832(6)$ Å, $\alpha = 97.44(1)°$, $\beta = 118.69(1)°$, $\gamma = 104.66(1)°$
Unit cell volume	104.39(3) Å^3
Temperature	294(1) K
d (calc)	2.48 g cm^{-3}
μ	1.42 mm^{-1}
Diffractometer	Enraf - Nonius CAD-4
Radiation	MoK_α, $\lambda = 0.71069$ Å
θ max	35°
Scan technique	$\omega/2\theta$
Reflections measured; unique reflections	1878; 896
Observed reflections	833 [$F_o > 4\sigma(F_o)$]
Absorption correction range	0.9975 0.8559
Function minimised	$\sum w\|\|F_o\|^2 - \|F_c\|^2\|^2$
Goodness-of-fit	1.050
Least squares weights	$1.0/[\sigma^2(F_o)^2 + (0.0945P)^2 + 0.0828P]$
Final R indices R, R_w	0.044 0.047
Max shift/esd (final cycle)	0.027

$R = \sum |F_o - F_c| / \sum F_o$

$R_w = \{\sum w(F_o - F_c)^2] / \sum w(F_o^2)\}^{1/2}$

Table 2. Positional and anisotropic displacement parameters (Å$\times 10^4$) for doyleite
$T = \exp[-2\pi^2(h^2a^{*2}U_{11} + k^2b^{*2}U_{22} + l^2c^{*2}U_{33} + 2klb^*c^*U_{23} + 2hla^*c^*U_{13} + 2hka^*b^*U_{12})]$.

Atom	x	y	z	U_{11}	U_{22}	U_{33}	U_{23}	U_{13}	U_{12}
Al	0.3269(1)	−0.0006(1)	0.1670(1)	98(3)	133(3)	114(3)	26(2)	59(2)	63(2)
O(1)	0.0868(3)	0.2090(2)	0.2016(3)	107(4)	122(4)	152(5)	7(3)	51(4)	61(4)
O(2)	0.7223(2)	0.2149(2)	0.5663(3)	99(4)	133(4)	137(4)	26(3)	63(4)	49(3)
O(3)	0.4672(3)	0.2107(2)	−0.0550(2)	144(4)	117(4)	148(4)	44(3)	100(4)	82(3)
H(1a)	0.16	0.40	0.30						
H(2a)	0.88	0.40	0.64						
H(3a)	0.56	0.40	0.00						
H(1b)	0.16	0.18	0.40						
H(2b)	0.88	0.18	0.52						
H(3b)	0.32	0.18	−0.26						

thermal parameters was by full-matrix least-squares minimising $\sum w||F_o|^2 - |F_c|^2|^2$. The final weights were $1.0/[\sigma^2(F_o) + (0.0945P)^2 + 0.0828P]$, where $P = [(F_o)^2 + 2F_c)^2]/3$, and the residual at convergence was 0.044.

Full crystal data and experimental and refinement details are summarised in Table 1. Atomic form factors are from International Tables for X-ray Crystallography, Vol. IV. The refinement program employed was SHELXL-96 (Sheldrick, 1996). Final atomic positions are listed in Table 2; bond distances and angles in Table 3.

Table 3. Bond distances (Å) and angles (°) for doyleite.

Al–O	Al–O(1)	1.858(1)	O–H	O(1)–H(1a)	0.932
	Al–O(2)	1.909(1)		O(2)–H(2a)	0.960
	Al–O(3)	1.892(1)		O(3)–H(3a)	0.909
	Al–O(1′)	1.877(1)		O(1)–H(1b)	0.923
	Al–O(2′)	1.900(1)		O(2)–H(2b)	0.971
	Al–O(3′)	1.873(1)		O(3)–H(3b)	0.887

O(1′) is related to O(1) through the centre of symmetry at (0,0,0)
O(2′) is related to O(2) through the centre of symmetry at ($^1/_2$,0,$^1/_2$)
O(3′) is related to O(3) through the centre of symmetry at ($^1/_2$,0,0)

Edges of the coordination octahedron

O–O			
O(1)–O(2)	2.803(1)	O(3)–O(1′)	2.741(1)
O(1)–O(3)	2.729(1)	O(1′)–O(2′)	2.791(1)
O(1)–O(1′)	2.389(1)	O(3′)–O(2)	2.721(1)
O(1)–O(2′)	2.775(1)	O(3′)–O(3)	2.376(1)
O(2)–O(3)	2.719(1)	O(3′)–O(1′)	2.729(1)
O(2)–O(2′)	2.454(1)	O(3′)–O(2′)	2.738(1)

Angles within the coordination octahedron

O(1)–Al–O(2)	95.63(5)	O(2)–Al–O(3′)	92.00(5)
O(1)–Al–O(3)	94.50(5)	O(3)–Al–O(1′)	93.33(5)
O(1)–Al–O(1′)	79.52(5)	O(3)–Al–O(2′)	167.74(5)
O(1)–Al–O(2′)	95.17(5)	O(3)–Al–O(3′)	78.28(5)
O(1)–Al–O(3′)	169.64(6)	O(1′)–Al–O(2′)	95.83(6)
O(2)–Al–O(3)	91.35(5)	O(1′)–Al–O(3′)	93.36(5)
O(2)–Al–O(1′)	173.50(5)	O(2′)–Al–O(3′)	93.02(5)
O(2)–Al–O(2′)	80.21(5)		

Edges of the trigonal prism of oxygen atoms between the layers

O(1)–O(2″)	2.775(1)	O(3)–O(3″)	2.874(1)
O(2)–O(1″)	2.775(1)		

O(1″) is related to O(1) through the centre of symmetry at ($^1/_2$, $^1/_2$, $^1/_2$)
O(2″) is related to O(2) through the centre of symmetry at ($^1/_2$, $^1/_2$, $^1/_2$)
O(3″) is related to O(3) through the centre of symmetry at ($^1/_2$, $^1/_2$, 0)

Atomic Force Microscopy

The surface of doyleite was examined using a Digital Instruments (DI) Nasoscope III Atomic Force Microscope (AFM). Images were obtained of the (010) cleavage plane in distilled water using a DI fluid cell and 100 μm wide leg cantilevers with integrated pyramidal silicon nitride tips. A 0.7 μm scan head was used and data collected in both constant height and constant force modes. The tracking force was minimized and estimated to be $1-5 \times 10^{-9}$ N. Samples were fixed on magnetized stainless steel supports using epoxy resin. The raw images have been filtered with a two dimensional fast Fourier algorithm (2DFFT) and all images proved reproducible under varying scan directions, contact force and tips.

A typical image of doyleite's (010) surface is shown in Fig. 2 along with an overlay of the structure calculated from the crystallographic data. There is good correspondence between the calculated structure and the AFM image. The dark regions correspond to cation vacancies with the brighter chain-like patterns of triangular $Al(OH)_3$ groups. The measured cross chain distance is 5.17 Å versus the 5.19 Å calculated from the crystallographic data.

Enzel and Henderson (1996) have demonstrated a very close agreement between the imaged surfaces of gibbsite, nordstrandite and doyleite and the calculated bulk struc-

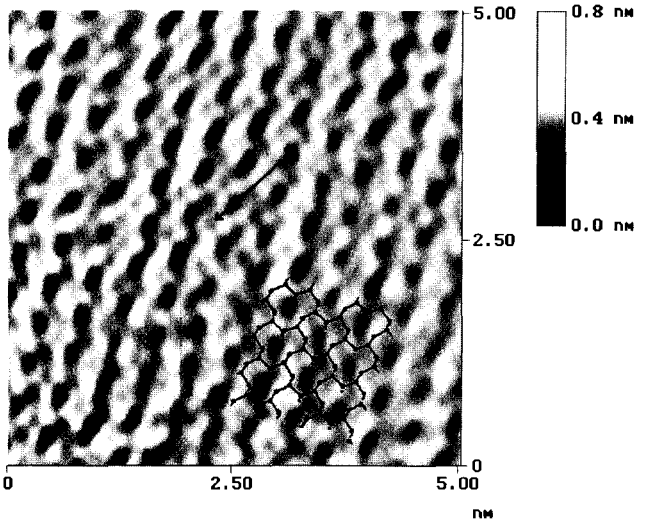

Fig. 2. A 2DFFT filtered AFM image of the (010) surface of doyleite imaged in a fluid cell. The structural overlay has been calculated for the doyleite structure with the protons in the horizontal plane only.

ture of gibbsite. However, their study did not take into consideration the possibility of hydrogens occupying different positions within the doyleite structure. Comparison of the present Fig. 2 with Fig. 2 of Enzel and Henderson (1996) shows significant differences. In their image of the nordstrandite surface a significant number of circular features exist that correspond closely to in-plane OH groups of the calculated structure. Fewer of these features, labelled as "a" in the present Fig. 2, exist in the doyleite images. Their relative scarcity accords with the interpretation of the protons of the OH groups occupying both intra-layer and inter-layer positions in doyleite. Fewer intra-layer features are observed in the AFM images as at any instant of time, a significant number of protons are in the vertical direction and are thus unable to be seen on the time scale of the AFM equipment.

Laser Raman Spectroscopy

The laser Raman spectra of transparent cleavages, 25 μm across, from a small granular crystal cluster supplied by Dr Chao as well as the crystal used for X-ray diffraction were recorded from 3000 cm^{-1} to 3900 cm^{-1} using a Jobin-Yvon U1000 spectrometer with Ar^+ as the exciting line operating at 514.5 nm and incident power of 500 mW–750 mW. Spectral bandpass was 500 μm, integration time was 1 sec for each incremental step of 1 cm^{-1}. An uncoated × 50 objective of an Olympus microscope was used for microsampling, the conventional arrangement of stage and lens giving 180E scattering geometry. Monochannel Ga-As photo-multiplier detectors (Burle C31034A) were employed operating at 243 K and 1800 V.

The Raman spectrum of doyleite is distinctive among the $Al(OH)_3$ polymorphs (Rodgers, 1992). Unlike the three to four scattering bands seen in the OH-stretching region in the spectra of gibbsite, bayerite and nordstrandite, doyleite displays a single broad (~ 100 cm^{-1} wide) band centred at about 3548 cm^{-1}. A weaker, but similarly

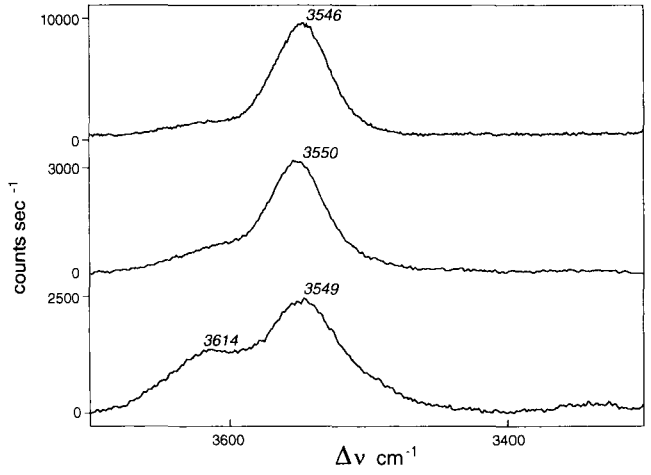

Fig. 3. Typical laser Raman spectra in the ν (OH)-stretching region from 3300 cm^{-1}–3700 cm^{-1} of fragments of doyleite crystals from Mt Saint-Hilaire, Quebec, microsampled on a glass mount. Intensities have been rescaled to arbitrary zero offset.

broad side band or shoulder at 3615 cm^{-1} occurs in some spectra (Fig. 3).

Chao et al., (1985) regarded the simplicity of the vibrational spectrum of doyleite as a consequence of the mineral having only one $Al(OH)_6$ octahedral grouping in its structure, unlike the other $Al(OH)_3$ polymorphs. The principal OH-stretching scattering behaviour reported here is seen as consistent with all the inter-layer OH groups possessing similar environments throughout the structure and, consequently having a limited range of vibrational modes.

The stretching frequencies of hydrogen-bonded OH groups are sensitive to the strength of the hydrogen bond and, in general, an observed band profile describes the convolution of all spectral functions related to a given broadening mechanism. The appreciable breadth of and general profile of doyleite's OH-stretching band shows similarities to those described from H_2O and D_2O whose inhomogenously broadened vibrational bands have been interpreted as arising from a distribution of varying hydrogen bond strengths having varying peak band frequencies (e.g. Pimentel and McClellan, 1960). Models having a continuous distribution of hydrogen bond strengths, or a disordered arrangement of a finite number of different species within the structure, have been proposed to satisfy the observed spectral behaviour (e.g. Eisenberg and Kauzmann, 1969). By analogy, in doyleite, the band broadening might then describe, to a first approximation, the time-averaged hydrogen bond-strength distribution throughout that area of the crystal being microprobed (cf. Fujita and Ikawa, 1989), with a continuous range of bond strengths consequential upon the interchanging positional disorder of the hydrogen atoms and their varying involvement in interplanar hydrogen bonds.

The subdued 3615 cm^{-1} side band of doyleite may relate to weak intra-layer interactions between hydroxyls. The precise nature of any bonding between a hydrogen and the next-nearest-neighbour oxygen within the layers is not clear and such interactions may be akin to those deduced for brucite where OH ... OH bonds are considered to involve no more than weak dipole-dipole interactions (e.g. Bragg et al., 1965).

Discussion

The structure of doyleite closely resembles those of the other $Al(OH)_3$ polymorphs, gibbsite, bayerite and nordstrandite, where Al^{3+} ions occupy two-thirds of the octahedral interstices within double layers of OH^- ions. The four polymorphs differ in the relative disposition of the double layers, and in the hydrogen bonding between and within the layers. The overall Al and O positions in doyleite were correctly predicted by Chao et al., (1985) on the basis of similarities in X-ray precession photographs in two zones compared with gibbsite and nordstrandite. The stacking of the double layers can be summarised as:

– in bayerite, each layer is stacked directly above the layer below in an *-AB-AB-AB-* sequence (where *A* represents the close-packed oxygen layer above the Al atoms, *B* represents the close-packed oxygen layer below the Al atoms, and the combination *AB*

represents one oxygen double layer (Zigan, Joswig and Burger, 1978);
- in gibbsite, each alternate double layer is turned upside down in an *-AB-BA-AB-* sequence (Saalfeld and Wedde, 1974);
- in nordstrandite, the stacking is *-AB-AB-AB-* as in bayerite, but with an accompanying shift of 1.82 Å along a direction inclined approximately 35° to the bayerite *a* axis (Bosmans, 1970);
- in doyleite the stacking is again *-AB-AB-AB-* but the lateral displacement is approximately at right angles to that of nordstrandite, being at 25° to the *b*-axis of bayerite.

If doyleite lacks well-defined intra-layer hydrogen bonds, as the evidence presented here would seem to suggest, it is the sole $Al(OH)_3$ polymorphs to do so. The crystal structure determinations of bayerite and gibbsite allowed all hydrogen atoms to be reliably located and established the presence of both inter- and intra-layer hydrogen bonding. Although the precise position of the hydrogen bonds has not be deduced for the nordstrandite structure, the OH-stretching behaviour is consistent with the existence of both inter- and intra-layer hydrogen bonds (Rodgers, 1992). The additional Raman scattering bands in the OH-stretching region of the spectra of bayerite, gibbsite and nordstrandite are presumably due to the intra-layer hydrogen bonds (both conventional and bifurcated) reported to exist in these polymorphs (e.g. Zigan, Joswig and Burger, 1978).

In the case of brucite, with its very weak OH ... OH interaction, Sherman (1991) argues that there is no delocalization of a hydrogen wave function onto the next-nearest neighbour oxygen as occurs where strong H-bonding is present, i.e. in those phases in which the metal-O bond is markedly covalent. The apparent absence of intra-layer hydrogen bonding in doyleite might then indicate that the strength of the Al–O covalent bond is insufficient to lower the charge on the O atom and weaken the O–H bond such that, in turn, the H ··· O bond becomes enhanced (cf. Sherman, 1991). The relative rarity of doyleite in nature and its inherent instability at ambient temperature and pressure may be an expression of the absence in the mineral of intra-layer hydrogen bonds.

References

Bosmans, H. J.: Unit cell and crystal structure of nordstrandite, $Al(OH)_3$. Acta Crystallogr. B**26** (1970) 649–652.

Chao, G. Y.; Baker, J.; Sabina, A. P.; Roberts, A. C.: Doyleite, a new polymorph of $Al(OH)_3$, and its relationship to bayerite, gibbsite and nordstrandite. Can. Mineral. **23** (1985) 21–28.

Eisenberg, D.; Kauzmann, W.: The structure and properties of water. Claredon, Oxford 1969.

Enzel, P. A.; Henderson, G. S.: AFM imaging of aluminium hydroxide surfaces. Scanning Micr. in press.

Fujita, Y.; Ikawa, S.: Effect of temperature on the hydrogen bond distribution in water as studied by infrared spectra. Chem. Phys. Lett. **159** (1989) 184–188.

International tables for X-ray crystallography, Vol. IV. (Eds. Ibers, J. A., Hamilton, W. C.) Birmingham, Knoch Press 1974.

North, A. C. T.; Phillips, D. C.; Mathews, F. S.: A semi-empirical method of absorption correction. Acta Crystallogr. A**24** (1968) 351–359.

Peterson, S. W.; Levy, H. A.: A single crystal diffraction study of heavy ice. Acta Crystallogr. **10** (1957) 70–76.

Pimentel, G. C.; McClellan, A. L.: The hydrogen bond. Freeman, San Francisco 1960.

Rodgers, K. A.: Routine identification of aluminium polymorphs with the laser Raman microprobe. Clay Miner. **28** (1992) 85–99.

Saalfeld, H.; Wedde, M.: Refinement of the crystal structure of gibbsite, $Al(OH)_3$. Z. Kristallogr. **139** (1974) 129–135.

Sheldrick, G. M.: SHELXS-86. Program for crystal structure determination. University of Göttingen, Germany 1986.

Sheldrick, G. M.: SHELXL-96. Program for refinement of crystal structures. University of Göttingen, Germany, 1996.

Sherman, D. M.: Hartree-Fock band structure, equation of state, and pressure-induced hydrogen bonding in brucite, $Mg(OH)_2$. Am. Mineral. **76** (1991) 1769–1772.

Wefers, K.; Misra, C.: Oxides and hydroxides of aluminum. Aloca Tech. Pap. **19** (1985) 1–92.

Zigan, F.; Joswig, W.; Burger, N.: Die Wasserstoffpositionen im Bayerit, $Al(OH)_3$. Z. Kristallogr. **148** (1978) 255–273.